Proceedings 10th NUMGE 2023
10th European Conference on Numerical Methods in Geotechnical Engineering
Zdravkovic L, Kontoe S, Taborda DMG, Tsiampousi A (eds)

https://doi.org/10.53243/NUMGE2023-75

Moving least squares material point method for porous media

A. Chmelnizkij[1]

[1] *Institute of Geotechnical Engineering and Construction Management, Hamburg University of Technology, Hamburg, Germany*

ABSTRACT: Different authors successfully applied the Moving Least Squares approximation (MLS) in the Material Point Method (MPM). In particular, the MLS provides better results for scattered distributions of material points than standard MPM approaches. The application of MLS to a coupled formulation, as in the case of saturated soil, bears further challenges. The transfer of information from material points to grid nodes and vice versa is performed on two material point sets, leading to different approximation accuracies for solid and liquid. This issue is investigated based on coupled wave propagation with randomly distributed material points. In the case of gaps in the distribution of material points, undesired reflections appear, which can affect the simulation results of dynamic problems such as pile installation, dynamic compaction, etc. in an unfavorable way. These reflections can be partly avoided by using MLS with large compact supports for the weighting functions. The best combinations of weighting functions are studied to improve the simulations.

Keywords: Material Point Method; Moving Least Squares; Coupled Wave Propagation

1 INTRODUCTION

The Material Point Method (MPM) originates from the Particle in Cell Method (PIC) introduced by Harlow (1962) for fluid mechanics. The Standard MPM introduced by Sulsky et al. (1994) further developed the ideas of PIC for solids. The application of PIC and MPM for geotechnical problems was first shown by Coetzee (2004) and Coetzee et al. (2005). Więckowski (2013) and Kafaji (2013) used MPM to model the dynamic behavior of water-saturated soil. Many other developments since then have further improved the MPM in its accuracy and stability and can be found in a summarized form in de Vaucorbeil (2020).

2 GEOTECHNICAL APPLICATIONS

There are a variety of applications in geotechnical engineering that involve large deformations and wave propagation. In most cases, waves are initiated in the area of large deformations and propagate over further distances. Examples may include pile driving, dynamic compaction, or subsurface explosions. The latter illustrates the problem particularly well. As shown in Figure 1, an underground explosion causes large deformations around the explosive charge, sometimes leading to craters on the surface. In addition to these de-

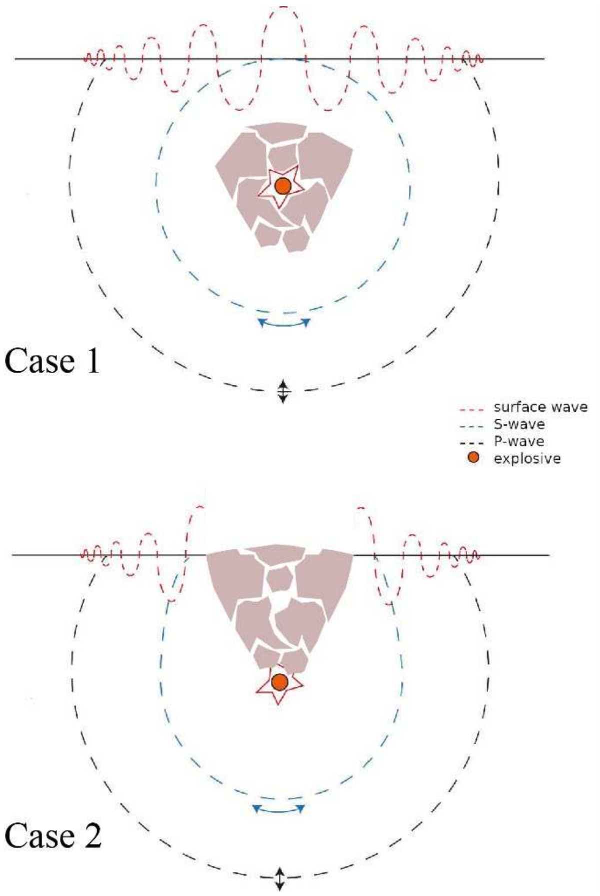

Figure 1 Schematic representation of subsurface explosions with (case 1) and without (case 2) craters at the surface.

formations, pressure, shear, and surface waves are induced.

Numerical simulation of such geotechnical boundary value problems imposes some requirements on the methods and formulations used. In the following, we present MPM as a suitable method and apply it to a coupled dynamic formulation for saturated soil.

3 MLS-MPM

MPM is a method suitable for simulations of large deformations. The usual Gaussian integration in the finite element method (FEM) is replaced by particle integration. This approach avoids the numerical integration of highly distorted elements, which leads to undesirable errors. Nevertheless, the standard MPM suffers from numerous other problems that can lead to stress oscillations and divergence. In the following, we will focus on two of these problems, the so-called grid-crossing and numerical fracture problems.

The grid-crossing problem in the standard MPM arises from the use of linear shape functions whose gradients are discontinuous along the element boundaries. This leads to oscillations in the calculation of internal forces by particle integration when a material point crosses from one element to another. The first approach to address this problem was made by introducing the Generalized Interpolation Material Point Method (GIMP) in Bardenhagen et al. (2004). Later, further developments to deal with the grid-crossing error led to the development of numerous MPM variants. In the following, we will concentrate on the use of B-splines as shape functions, which was first introduced by Steffen et al. (2008). B-Splines of quadratic and higher order possess continuous derivatives which mitigate the grid-crossing issue.

The numerical fracture problem has its origin in the finite domain of influence of the material points or in the compact support of the shape functions. In the case of the standard MPM, this means that as soon as an empty element is created by deformation, the material experiences a crack through which no information is transmitted. This cracking in the material is often undesirable since it depends only on the element size and thus has no direct physical significance. Since the higher order B-spline has a larger compact support, this error can also be partially avoided. Based on the work of Sulsky et al. (2016), we additionally use the Moving Least Square (MLS) approximation, which leads to higher accuracy in approximating the information between material points and nodes as well as vice versa. The MLS is a weighted least squares approximation based on weight functions and polynomial bases of different orders. For a vector $u = (u_1\ u_2\ \dots\ u_n)^T$ of n given values, the MLS approximation at $\mathbf{x}$ can be written as,

$$\Phi^{MLS}(x)u = \sum_{i=1}^{n} \Phi_i^{MLS}(x)u_i \tag{1}$$

with $\Phi_i^{MLS}(x) = w(x - \tilde{x}_i)\boldsymbol{p^T}(\boldsymbol{x})\boldsymbol{M^{-1}}(\boldsymbol{x})(\tilde{x}_i)$, where $p(x) = (1\ x\ y\ \dots\ xyz\ \dots)^T$ is a vector representing the polynomial basis of a desired order, $w(\boldsymbol{x} - \tilde{\boldsymbol{x}}_i)$ is the weighting function around $\tilde{\boldsymbol{x}}_i$ and $\mathbf{M}(\boldsymbol{x})$ the so-called moment matrix, which is formed from the weighting functions and the polynomial bases evaluated at the given values (Belytschko et al., 1996).
In the following, the MLS was applied to compute the nodal masses, velocities, and internal forces, while the remaining quantities were transferred using linear shape functions.

4 COUPLED FORMULATION

We now use the approximation presented in the previous section for a coupled formulation for saturated soil. The detailed derivation and discretization of the equations can be taken from Więckowski (2013) or Chmelnizkij (2023) and will be presented here only briefly. The two unknown vector fields are the velocities of the soil $\boldsymbol{v}_s$ and the pore fluid $\boldsymbol{v}_f$. Under the assumption of conservation of momentum, coupled partial differential equations can be considered,

$$n_s\rho_s \frac{D^s\boldsymbol{v}_s}{\mathrm{D}t} = \boldsymbol{\nabla}\cdot\boldsymbol{\sigma}' - \boldsymbol{\nabla}(n_s\, p_f) + n_s\rho_s\boldsymbol{b} - \boldsymbol{f_d}, \tag{2}$$

$$n_f\rho_f \frac{D^f\boldsymbol{v}_f}{\mathrm{D}t} = -\boldsymbol{\nabla}(n_f\, p_f) + n_f\rho_f\boldsymbol{b} + \boldsymbol{f_d}\ . \tag{3}$$

The following table gives an overview of the different quantities in Equations (2) and (3).

Table 1. Parameters, constants and variables in Equations (2) and (3)

$\boldsymbol{n_s}$	volume fraction (soil) [-]
$\boldsymbol{n_f}$	volume fraction (fluid) [-]
$\boldsymbol{\rho_s}$	grain density [kg/m³]
$\boldsymbol{\rho_f}$	fluid density [kg/m³]
$\boldsymbol{\sigma'}$	effective stress tensor [Pa]
$\boldsymbol{p_f}$	pore fluid pressure [Pa]
$\boldsymbol{b}$	body force [N]
$\boldsymbol{f_d}$	drag force [N]

The drag force represents the coupling between the soil and pore fluid and is assumed according to Darcy

$$\boldsymbol{f_d} = -n_f^2 \frac{\mu}{\kappa}(\boldsymbol{v_f} - \boldsymbol{v_s}), \tag{4}$$

where μ is the dynmaic viscosity and κ the instrinsic permeability. In the following, the body force $\boldsymbol{b}$ is assumed to be zero.

5 NUMERICAL RESULTS

To investigate the presented methods, we consider the wave propagation in a water-saturated column. The material parameters as well as further details of the boundary value problem can be taken from Chmelnizkij et al. (2019). First, we consider a random distribution of material points for the fluid and solid but without empty elements. The random distribution was generated in MATLAB using the *rand* function, which generates uniformly distributed random x-coordinates for the material points. Figure 2 shows the boundary value problem with the corresponding boundary conditions and the random distribution of the material points. As initial conditions the velocities of the fluid and solid are set to zero. The analytical solution to the problem can be found in Verruijt (2010). In the following we consider in particular the effective stress and the pore water pressure. The simulations were carried out with different weighting functions for a constant polynomial basis.

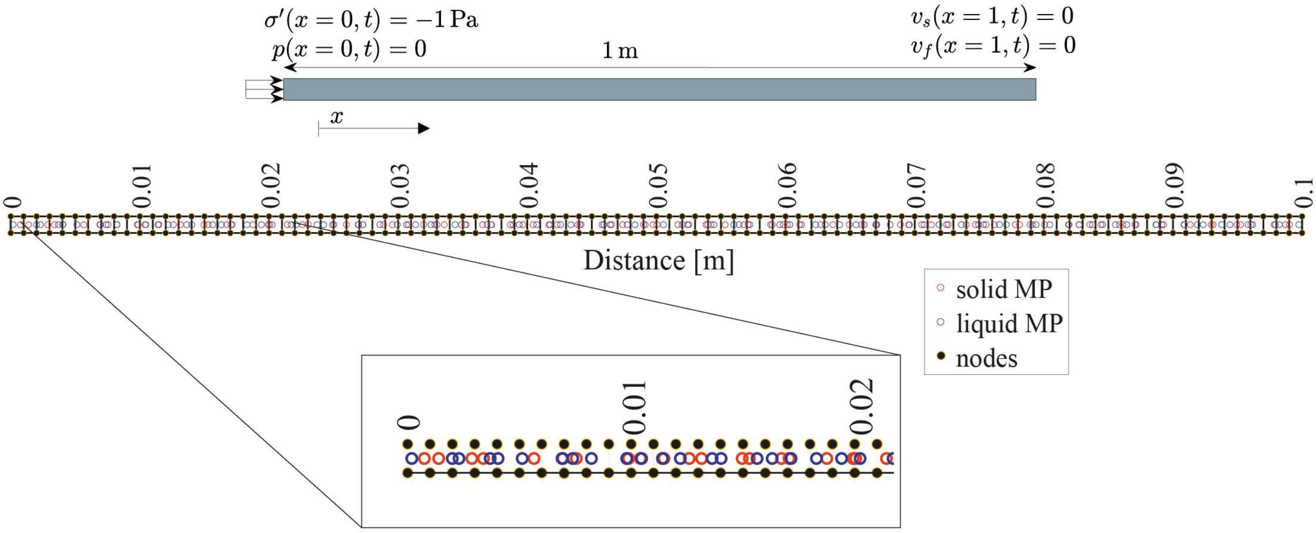

Figure 2 Boundary value problem with a scattered material point discretization for the soil and liquid.

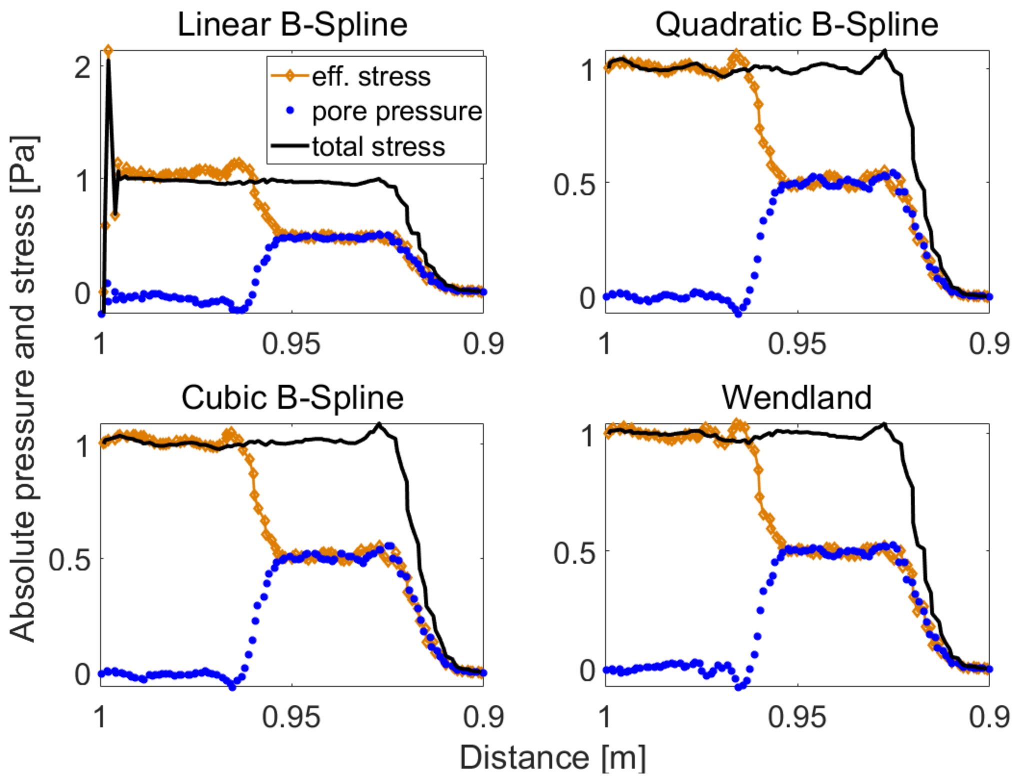

Figure 3 Comparison of different weighting functions.

The results in Figure 3 represent the numerical solution for different weighting functions after $t = 4 \cdot 10^{-5}$ s. Here, a positive pressure represents compression and a negative pressure represents tension. In addition to the B-splines, the Wendland function, as described in Chmelnizkij (2023) was used as a weighting function. It can be seen that when the linear shape function is used, there are large oscillations at the left boundary of the column due to the unfavourable distribution of the material points. The use of higher order B-splines and the Wendland function provide much better results.

In the next step, we consider the same column, now with a uniform distribution of material points but an empty element at x=0.05 m.

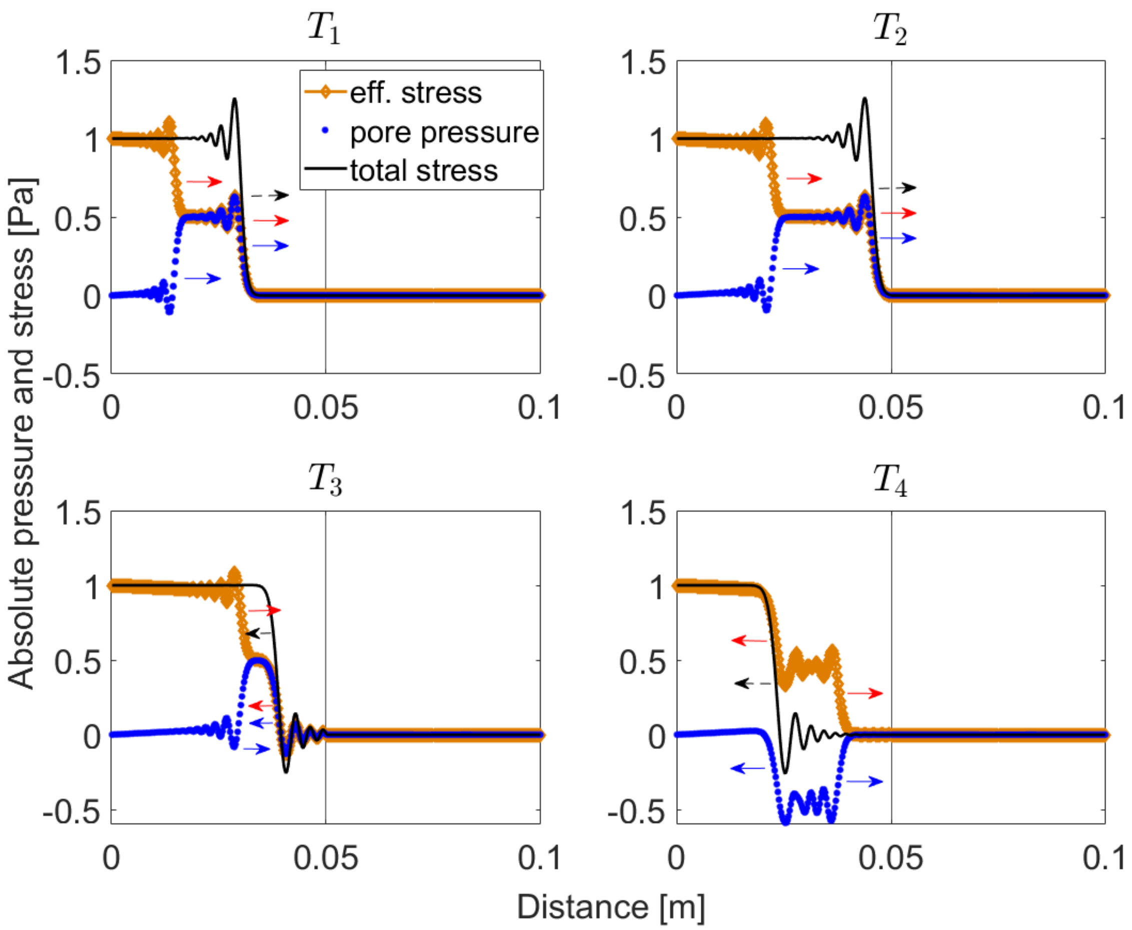

Figure 4 Results for the linear B-Spline weighting function at four consecutive time instants with a reflection from the empty element.

Figure 4 shows the results for wave propagation in a column with an empty element in the centre. Linear B-splines were used as the weighting function. The empty element acts like a loose end where the incident wave is reflected. No information arrives to the right of the empty element. This scenario can easily occur in a simulation with large deformations and lead to such numerical cracks, which are not physically justified. To reduce or avoid these reflections, weighting functions with larger compact supports can be chosen. The fact that the weighting functions are then also non-zero over a longer distance than one element means that the information can be transported across the gaps. In the following, we consider a calculation with the Wendland function and a compact support of 10 element lengths. Figure 5 shows the results of this calculation at four different time instants than Figure 4. Although the reflections cannot be suppressed completely and oscillations occur in the immediate vicinity of the gap, the results look much better compared to the absolute reflection in Figure 4. This shows that the presented approach can largely avoid the numerical fracture and associated reflections present in the standard MPM.

6 CONCLUSIONS

In this work, the MLS was used for a coupled dynamic formulation, and the shape function's compact support was chosen to be appropriately large to mitigate the reflexions and oscillations due to numerical fracture. While the grid-crossing problem does not arise directly in the wave propagation example shown, the MLS method allows for a variety of possible weighting functions, such as higher order B-splines or the Wendland functions shown, which allow for higher inter-element smoothness than C^0 and thus reduce the grid-crossing problem. The example of coupled wave propagation shows in a simplified way the phenomena that can occur in various dynamic simulations with large deformations. When simulating the underground explosions mentioned earlier using standard MPM, empty elements can appear immediately at the beginning, which makes it impossible to simulate correct wave propagation. Also, when simulating pile installations, impact- or vibratory-driven the generation of empty elements will lead to unphysical reflections. As we showed in the coupled wave propagation example, the MLS approach mitigates these reflections. It also increases the accuracy of MPM for randomly arranged material points, which is the preliminary stage of the formation of empty elements. promising application to the coupled wave propagation problem suggests that the method might also work for other applications with an adaptively chosen size of the compact support.

7 ACKNOWLEDGEMENTS

Funded by the Deutsche Forschungsgemeinschaft (DFG, German Research Foundation) – GR 1024/45

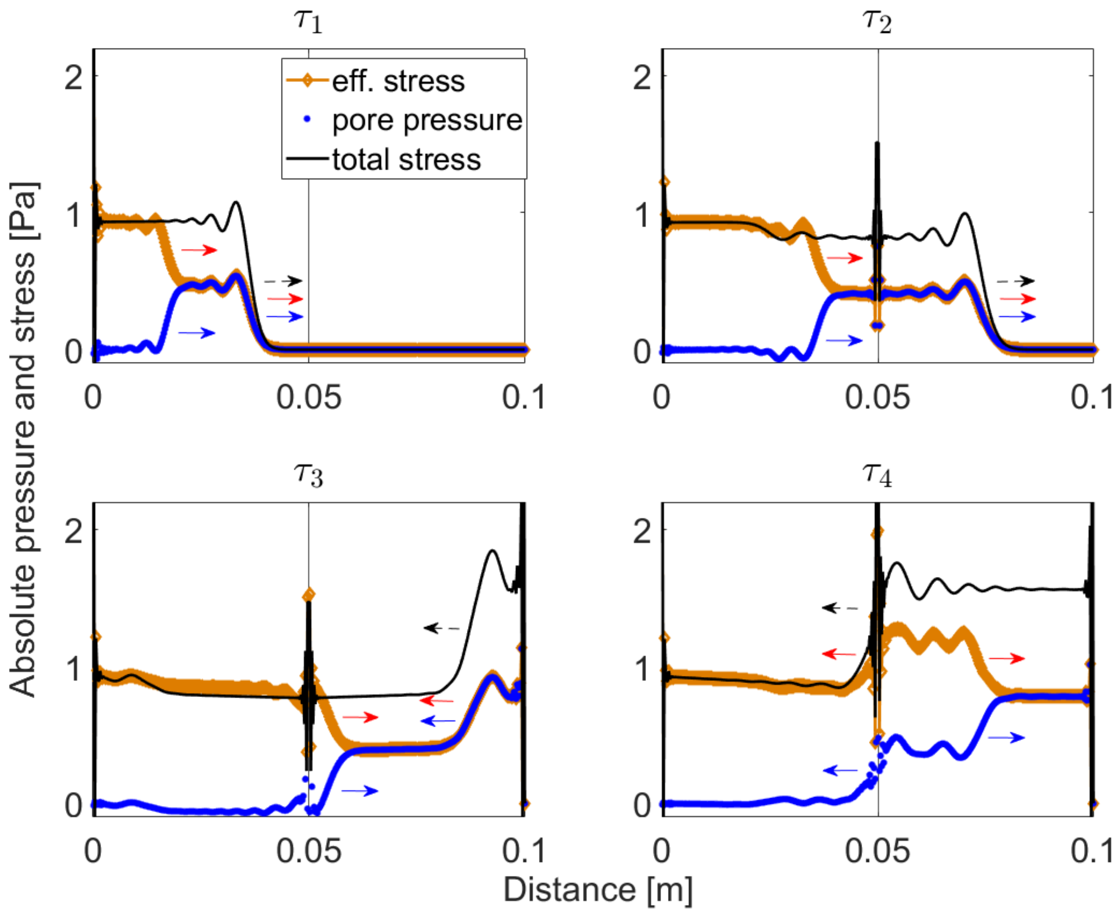

Figure 5 Results for the Wendland weighting function at four consecutive time instants.

8 REFERENCES

Al-Kafaji, I. 2013. *Formulation of a dynamic Material Point Method (MPM) for geomechanical problems.* Dissertation. Fakultät für Bau- und Umweltingenieurwissenschaften der Universität Stuttgart, Stuttgart, Germany.

Bardenhagen, S. & Kober, E. 2004. The Generalized Interpolation Material Point Method. *Computer Modeling in Engineering and Sciences*, **5(6)**, 477–495.

Belytschko, T., Krongauz, Y., Organ, D., Fleming, M., Krysl, P., 1996. Meshless methods: an overview and recent developments, *Computer methods in applied mechanics and engineering* **139(1-4)**, 3–47.

Chmelnizkij, A. 2023. *Regularized MPM for porous media* Dissertation. Institut für Geotechnik und Baubetrieb. Technische Universität Hamburg, Hamburg, Germany. https://doi.org/10.15480/882.4941

Chmelnizkij, A., F. Ceccato, J. Grabe, and P. Simonini (2019). 1D Wave propagation in saturated soils: verification of two-phase MPM. *In: 2nd International conference on the material point method for modelling soil-water-structure interaction.* Cambridge, UK.

Coetzee, C. J. 2004. *The modelling of granular flow using the particle-in-cell method*, Doctoral dissertation, University of Stellenbosch, Stellenbosch, South Africa.

Coetzee, C. J., Vermeer, P. A., & Basson, A. H. 2005. The modelling of anchors using the material point method. *International journal for numerical and analytical methods in geomechanics* **29(9)**, 879–895.

Harlow, F.H. 1962. *The particle-in-cell method for numerical solution of problems in fluid dynamics*. Los Alamos National Lab.(LANL), Los Alamos, NM (United States).

Steffen, M., Wallstedt, P., Guilkey, J., Kirby, R. and Berzins., M. Examination and analysis of implementation choices within the material point method (MPM). *Computer Modeling in Engineering and Sciences*, **31(2)**, 107–127.

Sulsky, D., Chen, Z., & Schreyer, H. L. 1994. A particle method for history-dependent materials. *Computer methods in applied mechanics and engineering* **118 (1-2)**, 179–196.

Sulsky, D. and Gong, M., 2016. Improving the material-point method, *Innovative Numerical Approaches for Multi-Field and Multi-Scale Problems*, pages 217–240. Springer, 2016.

de Vaucorbeil, A., Nguyen, V. P., Sinaie, S., & Wu, J. Y. 2020. Material point method after 25 years: Theory, implementation, and applications. *Advances in applied mechanics*, **53**, 185–398

Verruijt, A. 2010. *An intorduction to soil dynamics,* Springer, Berlin, Germany. https://doi.org/10.1007/978-90-481-3441-0

Więckowski, Z. 2013. *Enhancement of the material point method for fluid-structure interaction and erosion.* Research project report, Deltares, Delft, The Netherlands.